Z. Phys. C – Particles and Fields 53, 555–565 (1992)

Zeitschrift für Physik C Particles and Fields

Study of final state photons in hadronic Z^0 decay and limits on new phenomena

DELPHI Collaboration

P. Abreu[18], W. Adam[43], F. Adami[34], T. Adye[32], T. Akesson[21], G.D. Alekseev[13], P. Allen[42], S. Almehed[21], S.J. Alvsvaag[4], U. Amaldi[7], E. Anassontzis[3], P. Antilogus[22], W-D. Apel[14], R.J. Apsimon[32], B. Åsman[38], P. Astier[20], J-E. Augustin[16], A. Augustinus[27], P. Baillon[7], P. Bambade[16], F. Barao[18], R. Barate[11], G. Barbiellini[40], D.Y. Bardin[13], A. Baroncelli[35], O. Barring[21], W. Bartl[43], M.J. Bates[30], M. Battaglia[25], M. Baubillier[20], K-H. Becks[45], C.J. Beeston[30], M. Begalli[10], P. Beilliere[6], Yu. Belokopytov[37], P. Beltran[9], D. Benedic[8], J.M. Benlloch[42], M. Berggren[38], D. Bertrand[2], F. Bianchi[39], M.S. Bilenky[13], P. Billoir[20], J. Bjarne[21], D. Bloch[8], S. Blyth[30], V. Bocci[33], P.N. Bogolubov[13], T. Bolognese[34], M. Bonapart[27], M. Bonesini[25], W. Bonivento[25], P.S.L. Booth[19], M. Boratav[20], P. Borgeaud[34], G. Borisov[37], H. Borner[7], C. Bosio[35], B. Bostjancic[7], O. Botner[41], B. Bouquet[16], M. Bozzo[10], S. Braibant[2], P. Branchini[35], K.D. Brand[31], R.A. Brenner[12], C. Bricman[2], R.C.A. Brown[7], N. Brummer[27], J-M. Brunet[6], L. Bugge[29], T. Buran[29], H. Burmeister[7], J.A.M.A. Buytaert[7], M. Caccia[7], M. Calvi[25], A.J. Camacho Rozas[36], A. Campion[19], T. Camporesi[7], V. Canale[33], F. Cao[2], F. Carena[7], L. Carroll[19], C. Caso[10], E. Castelli[40], M.V. Castillo Gimenez[42], A. Cattai[7], F.R. Cavallo[5], L. Cerrito[33], A. Chan[1], M. Chapkin[37], P. Charpentier[7], P. Checchia[31], G.A. Chelkov[13], L. Chevalier[34], P. Chliapnikov[37], V. Chorowicz[20], R. Cirio[39], M.P. Clara[39], P. Collins[30], J.L. Contreras[23], R. Contri[10], G. Cosme[16], F. Couchot[16], H.B. Crawley[1], D. Crennell[32], G. Crosetti[10], M. Crozon[6], J. Cuevas Maestro[36], S. Czellar[12], S. Dagoret[16], E. Dahl-Jensen[26], B. Dalmagne[16], M. Dam[4], G. Damgaard[26], G. Darbo[10], E. Daubie[2], P.D. Dauncey[30], M. Davenport[7], P. David[20], A. De Angelis[40], M. De Beer[34], H. De Boeck[2], W. De Boer[14], C. De Clercq[2], M.D.M. De Fez Laso[42], N. De Groot[27], C. De La Vaissiere[20], B. De Lotto[40], A. De Min[25], C. Defoix[6], D. Delikaris[7], S. Delorme[7], P. Delpierre[6], N. Demaria[39], L. Di Ciaccio[33], H. Dijkstra[7], F. Djama[8], J. Dolbeau[6], O. Doll[45], M. Donszelmann[27], K. Doroba[44], M. Dracos[7], J. Drees[45], M. Dris[28], Y. Dufour[6], W. Dulinski[8], L-O. Eek[41], P.A.-M. Eerola[7], T. Ekelof[41], G. Ekspong[38], A. Elliot Peisert[31], J-P. Engel[8], D. Fassouliotis[28], M. Feindt[7], M. Fernandez Alonso[36], A. Ferrer[42], T.A. Filippas[28], A. Firestone[1], H. Foeth[7], E. Fokitis[28], P. Folegati[40], F. Fontanelli[10], K.A.J. Forbes[19], H. Forsbach[45], B. Franek[32], P. Frenkiel[6], D.C. Fries[14], A.G. Frodesen[4], R. Fruhwirth[43], F. Fulda-Quenzer[16], K. Furnival[19], H. Furstenau[14], J. Fuster[7], G. Galeazzi[31], D. Gamba[39], C. Garcia[42], J. Garcia[36], C. Gaspar[7], U. Gasparini[31], P. Gavillet[7], E.N. Gazis[28], J-P. Gerber[8], P. Giacomelli[7], K-W. Glitza[45], R. Gokieli[7], V.M. Golovatyuk[13], J.J. Gomez Y Cadenas[7], A. Goobar[38], G. Gopal[32], M. Gorski[44], V. Gracco[10], A. Grant[7], F. Grard[2], E. Graziani[35], M-H. Gros[16], G. Grosdidier[16], E. Gross[7], B. Grossetete[20], P. Grosse-Wiesmann[7], J. Guy[32], F. Hahn[7], M. Hahn[14], S. Haider[27], Z. Hajduk[15], A. Hakansson[21], A. Hallgren[41], K. Hamacher[45], G. Hamel De Monchenault[34], F.J. Harris[30], B.W. Heck[7], T. Henkes[7], I. Herbst[45], J.J. Hernandez[42], P. Herquet[2], H. Herr[7], I. Hietanen[12], C.O. Higgins[19], E. Higon[42], H.J. Hilke[7], S.D. Hodgson[30], T. Hofmokl[44], R. Holmes[1], S-O. Holmgren[38], D. Holthuizen[27], P.F. Honore[6], J.E. Hooper[26], M. Houlden[19], J. Hrubec[43], P.O. Hulth[38], K. Hultqvist[38], D. Husson[8], P. Ioannou[3], D. Isenhower[7], P-S. Iversen[4], J.N. Jackson[19], P. Jalocha[15], G. Jarlskog[21], P. Jarry[34], B. Jean-Marie[16], E.K. Johansson[38], D. Johnson[19], M. Jonker[7], L. Jonsson[21], P. Juillot[8], G. Kalkanis[3], G. Kalmus[32], F. Kapusta[20], S. Katsanevas[3], E.C. Katsoufis[28], R. Keranen[12], J. Kesteman[2], B.A. Khomenko[13], N.N. Khovanski[13], B. King[19], N.J. Kjaer[7], H. Klein[7], W. Klempt[7], A. Klovning[4], P. Kluit[27], A. Koch-Mehrin[45], J.H. Koehne[14], B. Koene[27], P. Kokkinias[9], M. Kopf[14], M. Koratzinos[39], K. Korcyl[15], A.V. Korytov[13], V. Kostukhin[37], C. Kourkoumelis[3], T. Kreuzberger[43], J. Krolikowski[44], I. Kronkvist[21], J. Krstic[30], U. Kruener-Marquis[45], W. Krupinski[15], W. Kucewicz[25], K. Kurvinen[12], C. Lacasta[42], C. Lambropoulos[9], J.W. Lamsa[1], L. Lanceri[40], V. Lapin[37], J-P. Laugier[34], R. Lauhakangas[12], G. Leder[43], F. Ledroit[11], R. Leitner[7], Y. Lemoigne[34], J. Lemonne[2], G. Lenzen[45], V. Lepeltier[16], A. Letessier-Selvon[20], D. Liko[43], E. Lieb[45], E. Lillethun[4], J. Lindgren[12], A. Lipniacka[44], I. Lippi[31], R. Llosa[23], B. Loerstad[21], M. Lokajicek[13], J.G. Loken[30], M.A. Lopez Aguera[36], A. Lopez-Fernandez[16], M. Los[27], D. Loukas[9], A. Lounis[8], J.J. Lozano[42], R. Lucock[32], P. Lutz[6], L. Lyons[30], G. Maehlum[7], N. Magnussen[45], J. Maillard[6], A. Maltezos[9], F. Mandl[43], J. Marco[36], M. Margoni[31], J-C. Marin[7], A. Markou[9], S. Marti[42], L. Mathis[6], F. Matorras[36], C. Matteuzzi[25], G. Matthiae[33], M. Mazzucato[31], M. McCubbin[19], R. McKay[1], R. McNulty[19], E. Menichetti[39], G. Meola[10], C. Meroni[25], W.T. Meyer[1], M. Michelotto[31], W.A. Mitaroff[43], G.V. Mitselmakher[13], U. Mjoernmark[21], T. Moa[38], R. Moeller[26], K. Moenig[7], M.R. Monge[10], P. Morettini[10], H. Mueller[14], W.J. Murray[32], G. Myatt[30], F. Naraghi[20], U. Nau-Korzen[45], F.L. Navarria[5], P. Negri[25], B.S. Nielsen[26], B. Nijjhar[19], V. Nikolaenko[37], V. Obraztsov[37], A.G. Olshevski[13],

R. Orava[12], A. Ostankov[37], A. Ouraou[34], M. Paganoni[25], R. Pain[20], H. Palka[27], T. Papadopoulou[28], L. Pape[7], A. Passeri[35], M. Pegoraro[31], V. Perevozchikov[37], M. Pernicka[43], A. Perrotta[5], F. Pierre[34], M. Pimenta[18], O. Pingot[2], M.E. Pol[7], G. Polok[15], P. Poropat[40], P. Privitera[14], A. Pullia[25], J. Pyyhtia[12], D. Radojicic[30], S. Ragazzi[25], P.N. Ratoff[17], A.L. Read[29], N.G. Redaelli[25], M. Regler[43], D. Reid[19], P.B. Renton[30], L.K. Resvanis[3], F. Richard[16], M. Richardson[19], J. Ridky[13], G. Rinaudo[39], I. Roditi[7], A. Romero[39], I. Roncagliolo[10], P. Ronchese[31], V. Ronjin[37], C. Ronnqvist[12], E.I. Rosenberg[1], U. Rossi[5], E. Rosso[7], P. Roudeau[16], T. Rovelli[5], W. Ruckstuhl[27], V. Ruhlmann[34], A. Ruiz[36], K. Rybicki[15], H. Saarikko[12], Y. Sacquin[34], G. Sajot[11], J. Salt[42], E. Sanchez[42], J. Sanchez[23], M. Sannino[10], M. Schaeffer[8], S. Schael[14], H. Schneider[14], M.A.E. Schyns[7], F. Scuri[40], A.M. Segar[30], R. Sekulin[32], M. Sessa[40], G. Sette[10], R. Seufert[14], R.C. Shellard[7], P. Siegrist[34], S. Simonetti[10], F. Simonetto[31], A.N. Sissakian[13], T.B. Skaali[29], G. Skjevling[29], G. Smadja[34,22], N. Smirnov[37], G.R. Smith[32], R. Sosnowski[44], T.S. Spasoff[11], E. Spiriti[35], S. Squarcia[10], H. Staeck[45], C. Stanescu[35], G. Stavropoulos[9], F. Stichelbaut[2], A. Stocchi[16], J. Strauss[43], R. Strub[8], M. Szczekowski[44], M. Szeptycka[44], P. Szymanski[44], T. Tabarelli[25], S. Tavernier[2], G.E. Theodosiou[9], A. Tilquin[24], J. Timmermans[27], V.G. Timofeev[13], L.G. Tkatchev[13], T. Todorov[13], D.Z. Toet[27], E. Torassa[39], L. Tortora[35], M.T. Trainor[30], D. Treille[7], U. Trevisan[10], W. Trischuk[7], G. Tristram[6], C. Troncon[25], A. Tsirou[7], E.N. Tsyganov[13], M. Turala[15], R. Turchetta[8], M-L. Turluer[34], T. Tuuva[12], I.A. Tyapkin[13], M. Tyndel[32], S. Tzamarias[7], B. Ueberschaer[45], S. Ueberschaer[45], O. Ullaland[7], V.A. Uvarov[37], G. Valenti[5], E. Vallazza[39], J.A. Valls Ferrer[42], G.W. Van Apeldoorn[27], P. Van Dam[27], W.K. Van Doninck[2], C. Vander Velde[2], J. Varela[18], P. Vaz[7], G. Vegni[25], L. Ventura[31], W. Venus[32], F. Verbeure[2], L.S. Vertogradov[13], L. Vibert[20], D. Vilanova[34], N. Vishnevsky[37], L. Vitale[40], E.V. Vlasov[37], S. Vlassopoulos[28], A.S. Vodopyanov[13], M. Vollmer[45], S. Volponi[5], G. Voulgaris[3], M. Voutilainen[12], V. Vrba[35], H. Wahlen[45], C. Walck[38], F. Waldner[40], M. Wayne[1], P. Weilhammer[7], J. Werner[45], A.M. Wetherell[7], J.H. Wickens[2], J. Wikne[29], G.R. Wilkinson[30], W.S.C. Williams[30], M. Winter[8], D. Wormald[29], G. Wormser[16], K. Woschnagg[41], N. Yamdagni[38], P. Yepes[7], A. Zaitsev[37], A. Zalewska[15], P. Zalewski[44], D. Zavrtanik[7], E. Zevgolatakos[9], G. Zhang[45], N.I. Zimin[13], M. Zito[34], R. Zitoun[20], R. Zukanovich Funchal[6], G. Zumerle[31], J. Zuniga[42]

[1] Ames Laboratory and Department of Physics, Iowa State University, Ames IA 50011, USA
[2] Physics Department, Univ. Instelling Antwerpen, Universiteitsplein 1, B-2610 Wilrijk, Belgium, and IIHE, ULB-VUB, Pleinlaan 2, B-1050 Brussels, Belgium, and Service de Phys. des Part. Elém. Faculté des Sciences, Université de l'Etat Mons, Av. Maistriau 19, B-7000 Mons, Belgium
[3] Physics Laboratory, University of Athens, Solonos Str. 104, GR-10680 Athens, Greece
[4] Department of Physics, University of Bergen, Allégaten 55, N-5007 Bergen, Norway
[5] Dipartimento di Fisica, Università di Bologna and INFN, Via Irnerio 46, I-40126 Bologna, Italy
[6] Collège de France, Lab. de Physique Corpusculaire, 11 pl. M. Berthelot, F-75231 Paris Cedex 05, France
[7] CERN, CH-1211 Geneva 23, Switzerland
[8] Division des Hautes Energies, CRN – Groupe DELPHI and LEPSI, B.P.20CRO, F-67037 Strasbourg Cedex, France
[9] Institute of Nuclear Physics, N.C.S.R. Demokritos, P.O. Box 60228, GR-15310 Athens, Greece
[10] Dipartimento di Fisica, Università di Genova and INFN, Via Dodecaneso 33, I-16146 Genova, Italy
[11] Institut des Sciences Nucléaires, Université de Grenoble 1, F-38026 Grenoble, France
[12] Research Institute for High Energy Physics, University of Helsinki, Siltavuorenpenger 20C, SF-00170 Helsinki 17, Finland
[13] Joint Institute for Nuclear Research, Dubna, Head Post Office, P.O. Box 79, SU-101000 Moscow, USSR
[14] Institut für Experimentelle Kernphysik, Universität Karlsruhe, Postfach 6980, W-7500 Karlsruhe 1, Federal Republic of Germany
[15] High Energy Physics Laboratory, Institute of Nuclear Physics, Ul. Kawiory 26a, PL-30055 Krakow 30, Poland
[16] Université de Paris-Sud, Lab. de l'Accélérateur Linéaire, Bat 200, F-91405 Orsay, France
[17] School of Physics and Materials, University of Lancaster, Lancaster LA1 4YB, UK
[18] LIP, Av. Elias Garcia 14 – 1e, P-1000 Lisbon Codex, Portugal
[19] Department of Physics, University of Liverpool, P.O. Box 147, Liverpool L69 3BX, UK
[20] LPNHE, Universités Paris VI et VII, Tour 33 (RdC), 4 place Jussieu, F-75230 Paris Cedex 05, France
[21] Department of Physics, University of Lund, Sölvegatan 14, S-22363 Lund, Sweden
[22] Université Claude Bernard de Lyon, 43 Bd du 11 Novembre 1918, F-69622 Villeurbanne Cedex, France
[23] Universidad Complutense, Avda. Complutense s/n, E-28040 Madrid, Spain
[24] Univ. d'Aix – Marseille II – Case 907 – 70, route Léon Lachamp, F-13288 Marseille Cedex 09, France
[25] Dipartimento di Fisica, Università di Milano and INFN, Via Celoria 16, I-20133 Milan, Italy
[26] Niels Bohr Institute, Blegdamsvej 17, DK-2100 Copenhagen 0, Denmark
[27] NIKHEF-H, Postbus 41882, NL-1009 DB Amsterdam, The Netherlands
[28] National Technical University, Physics Department, Zografou Campus, GR-15773 Athens, Greece
[29] Physics Department, University of Oslo, Blindern, N-1000 Oslo 3, Norway
[30] Nuclear Physics Laboratory, University of Oxford, Keble Road, Oxford OX1 3RH, UK
[31] Dipartimento di Fisica, Università di Padova and INFN, Via Marzolo 8, I-35131 Padua, Italy
[32] Rutherford Appleton Laboratory, Chilton, Didcot OX11 OQX, UK
[33] Dipartimento di Fisica, Università di Roma II and INFN, Tor Vergata, I-00173 Rome, Italy
[34] CEN-Saclay, DPhPE, F-91191 Gif-sur-Yvette Cedex, France
[35] Istituto Superiore di Sanità, Ist. Naz. di Fisica Nucl. (INFN), Viale Regina Elena 299, I-00161 Rome, Italy
[36] Facultad de Ciencias, Universidad de Santander, av. de los Castros, E-39005 Santander, Spain
[37] Inst. for High Energy Physics, Serpukow P.O. Box 35, Protvino, (Moscow Region), USSR
[38] Institute of Physics, University of Stockholm, Vanadisvägen 9, S-11346 Stockholm, Sweden
[39] Dipartimento di Fisica Sperimentale, Università di Torino and INFN, Via P. Giuria 1, I-10125 Turin, Italy

[40] Dipartimento di Fisica, Università di Trieste and INFN, Via A. Valerio 2, I-34127 Trieste, Italy, and Istituto di Fisica, Università di Udine, I-33100 Udine, Italy
[41] Department of Radiation Sciences, University of Uppsala, P.O. Box 535, S-75121 Uppsala, Sweden
[42] Inst. de Fisica Corpuscular IFIC, Centro Mixto Univ. de Valencia-CSIC, and Departamento de Fisica Atomica Molecular y Nuclear, Univ. de Valencia, Avda. Dr. Moliner 50, E-46100 Burjassot (Valencia), Spain
[43] Institut für Hochenergiephysik, Österreich Akademie der Wissenschaften, Nikolsdorfergasse 18, A-1050 Vienna, Austria
[44] Inst. Nuclear Studies and University of Warsaw, Ul. Hoza 69, PL-00681 Warsaw, Poland
[45] Fachbereich Physik, University of Wuppertal, Postfach 100127, W-5600 Wuppertal 1, Federal Republic of Germany

Received 18 October 1991

Abstract. The differential cross section for final state radiation from primary quarks is obtained from a study of isolated energetic photons produced in the reaction $e^+e^- \to Z^0 \to \text{hadrons} + \gamma$, as measured in the DELPHI detector at the CERN LEP collider. When combined with the measurement of the total hadronic width of the Z^0, the observed rate determines the electroweak coupling constants of up and down type quarks, i.e.,

$$v_{1/3}^2 + a_{1/3}^2 = 1.13 \pm 0.29 \quad \text{and} \quad v_{2/3}^2 + a_{2/3}^2 = 1.65 \pm 0.43.$$

No evidence is seen for additional photon production from anomalous decays of the Z^0 or from decays of new particles. This measurement leads to upper limits on the production cross section times branching fraction of (a) the Higgs boson in the reaction $e^+e^- \to Z^0 \to H + \gamma$, $H \to$ hadrons, (b) an excited quark, $q^* \to q + \gamma$, and (c) the contribution of an anomalous decay of the Z^0 into a photon and hadrons. These limits, all at the 95% confidence level, vary from 3 to 10 pb as the mass of the intermediate state (H, q^* or Z^*) varies from 10 GeV/c^2 to 80 GeV/c^2.

1 Introduction

This paper presents a measurement of the differential cross section for the production of energetic isolated photons in the reaction $e^+e^- \to Z^0 \to \text{hadrons} + \gamma$ where the photon originates from final state radiation. Such prompt high energy photons may also arise from initial state radiation (ISR). In addition, significant background to such QED radiation processes is expected from (a) the decay of hadrons, mostly π^0's, produced in the fragmentation of the final state quarks (QCD), and (b) $\tau^+\tau^-$ decays of the Z^0.

After the subtraction of initial state radiation and of QCD fragmentation remnants, the properties of isolated energetic photons are found to be consistent with the expectation of final state photon radiation from quarks. This measurement is used to determine the weak couplings of up- and down-type quarks. The rate of final state radiation is expected to be proportional to the squares of the electric charges of the produced quarks [1], thus increasing the proportion of radiation from charge 2/3 quarks. The rate of final state radiation, when combined with the measured hadronic width of the Z^0, allows the determination of the electroweak couplings of up- and down-type quarks [2].

Isolated energetic photons may also originate from new particle production or from anomalous decays of the Z^0. For example, the production of an excited quark, q^*, and the process $Z^0 \to \text{Higgs} + \gamma$ [3] would lead to a similar signature. If the Z^0 boson were a composite particle, then its decay into an isolated energetic photon plus an off-mass-shell Z^0 (forbidden to all orders in the standard model) would be allowed [4].

2 The DELPHI detector

This analysis is based on the data collected with the DELPHI detector [5] at the CERN LEP collider in 1989 and 1990. The data were recorded at center of mass energies, $\sqrt{s}$, between 88.20 GeV and 94.22 GeV around the Z^0 pole with an integrated luminosity of about 4.7 pb^{-1}. Features of the DELPHI apparatus relevant for the analysis of multihadronic final states are outlined in [6]. The present analysis relies on the information provided both by the three cylindrical tracking detectors (inner detector, time projection chamber (TPC), and outer detector) and by the barrel electromagnetic calorimeter for photon detection, all operating in a 1.2 T magnetic field.

The inner detector and TPC each cover the angular range $20° < \vartheta < 160°$, where ϑ is the polar angle with respect to the beam axis, and the outer detectors covers the range $43° < \vartheta < 137°$.

Energetic isolated photons were detected in the high-density projection chamber (HPC) barrel electromagnetic calorimeter. The HPC subtends the angular range $41° < \vartheta < 139°$. It is mounted directly inside the 5.2 m (inner diameter) superconducting solenoid of DELPHI. It consists of 144 modules arranged in 24 azimuthal sectors, where each sector consists of six modules along the beam axis.

The HPC is a gas sampling calorimeter which uses a long drift time to provide complete three-dimensional charge information in the manner of a time-projection chamber. Each module consists of 40 layers of lead radiator totalling about 17 radiation lengths, interspersed with 39 gas sampling slots containing a mixture of argon and methane gases. Charge due to ionisation produced in the electromagnetic showers drifts longitudinally in parallel electric and magnetic fields, and is read out via a grid of cathode pads. The 15 MHz sampling frequency provides a cell size of 3.5 mm along the beam axis.

The HPC electromagnetic calorimeter has been described in the literature [7] as have the readout electron-

ics [8]. The energy resolution of the HPC has been determined from a study of the Bhabha events (45 GeV electromagnetic showers) plus about 700 Compton scatter events in which the scattered electron or positron produces an electromagnetic shower in the HPC, and the scattered photon is detected in the forward electromagnetic calorimeters. The electrons and positrons have energies predominantly in the range from 3 GeV to 15 GeV. The energy resolution of the HPC is consistent with $(\sigma/E)^2=(26\%/\sqrt{E})^2+(7\%)^2$ with E in GeV.

3 Event selection criteria

The detection of multihadronic events was accomplished entirely with charged particles, and is described in the DELPHI publications on the hadronic line shape [9].

The following selection criteria for charged particles were used:

(i) Polar angle ϑ between 20° and 160°.
(ii) Momentum p between 0.1 GeV/c and 50 GeV/c.
(iii) Track length above 30 cm.
(iv) Relative error on momentum measurement below 100%.
(v) Projection of impact parameter with respect to the beam in the plane perpendicular to the beam axis below 4 cm.
(vi) Longitudinal coordinate at the origin below 10 cm.

Hadronic events were then selected by requiring at least eight charged particle tracks, or at least three charged particle tracks of momenta greater than 2 GeV/c each, all contained within a cone of opening angle at most 100°.

The multiplicity cut removed cosmic ray events and leptonic decays with the exception of a small contribution from $\tau^+\tau^-$ events. The cone requirement reduced the contamination by beam gas events and events due to two photon interactions to a negligible level.

With the above criteria, 98% of all true hadronic events and 31% of all $\tau^+\tau^-$ events were included. Thus, the event sample consisted of $(98.6\pm1.0)\%$ hadronic events and $(1.4\pm0.1)\%$ $\tau^+\tau^-$ decays.

Events with energetic isolated photons were selected from the sample of multihadronic events with at least the TPC and the HPC fully working and satisfying the cuts described above (in total 105876 events). The criteria for such photons were:

a) An electromagnetic shower in the HPC with polar angle, ϑ_γ, between 45° and 135°. This cut reduced considerably the contribution from initial state radiation.
b) The shower out of the region $88°<\vartheta_\gamma<92°$, as this is a region with mechanical supports.
c) The shower in the HPC with at least 8 GeV measured energy and not linked to an incident charged track. Showers are linked to extrapolated charged particle tracks if their spatial separation is less than 4 cm at the HPC entrance (radius = 208 cm).
d) An isolation angle of the shower axis with charged particle tracks at the Z^0 decay of at least 20°. This means that the space angle between the candidate shower direction and the directions of all charged particle tracks of momentum greater than 0.5 GeV/c had to be greater than 20°.
e) An isolation angle of the shower axis with other neutral particles of at least 20°, i.e. the space angle between the candidate shower direction and the directions of all other neutrals of energy greater than 2 GeV had to be greater than 20°.
f) Because of poor efficiency for shower detection at the edges of HPC modules, and because of the possibility that an energetic electron in a crack between TPC sectors will fail to produce a charged particle track but will produce an electromagnetic shower in the HPC, thus simulating a photon, fiducial cuts in azimuth were also imposed. These were $\pm1°$ in azimuth at each of the 24 HPC module boundaries and $\pm1°$ in azimuth at each of the 6 TPC sector boundaries.

A total of 401 events satisfied the above criteria for multihadronic events with isolated energetic photons.

To further suppress photons from highly energetic neutral pions, which occur predominantly within jets, an additional cut on the transverse momentum, p_T, of the photon relative to the event thrust axis was also applied. The thrust axis was calculated using all the charged particles in the event, but not the neutral particles. The motivation for this cut on p_T is illustrated in Fig. 1, which shows the distribution of the transverse momentum with respect to the thrust axis for energetic isolated photons before applying the p_T cut. The spectrum extends up to p_T about 35 GeV/c. Also shown are

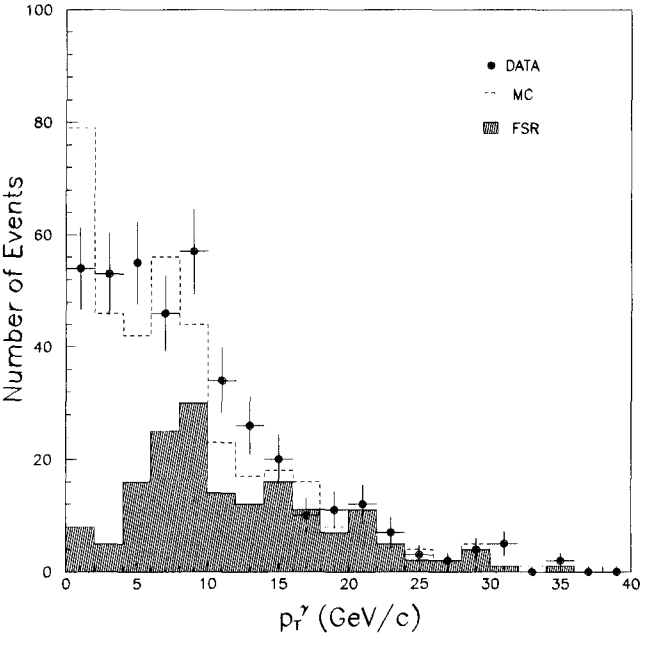

Fig. 1. Transverse momentum distribution of isolated energetic photons with respect to the event thrust axis, showing data (points with errors), simulation including only FSR (cross hatched area), and simulation including FSR plus the backgrounds from ISR, QCD and τ decays. The event thrust axis is calculated using all the charged particles in the event

the predictions of the Monte Carlo calculation for final state radiation (FSR), and for the background processes (ISR + QCD + τ) plus final state radiation. The background dominates the region $p_T < 5$ GeV/c. A cut of $p_T > 5$ GeV/c reduces the number of energetic isolated photons from background processes (ISR + QCD + τ) by more than a factor of two, but reduces the signal (FSR) by only 12%. A total of 262 events survived this cut. The Monte Carlo calculations indicate that the total background (ISR + QCD + τ) is reduced to 84 events with this cut. Also, in the region $p_T > 5$ GeV/c, the Monte Carlo prediction for background plus final state radiation agrees well with the observed data. The numbers of events surviving the various cuts and the corresponding predictions of the Monte Carlo simulation are shown in Table 1, which is discussed in detail in Sect. 5.

In addition, the theoretical expectations are that such a p_T cut reduces the probability of gluon bremsstrahlung from the primary quark occurring before the hard photon radiation [1].

4 Simulation of the background

The background to the observed candidate events, remaining after the above cuts, was estimated from Monte Carlo generation of the reaction $e^+ e^- \to Z^0 \to q\bar{q}$ [10].

For the parton generation, the parton shower option (PS [1]), based on a combination of the exact first order QCD matrix element and the leading log approximation (LLA), was used. This approximation is not valid for hard large-angle gluon radiation. Therefore the first gluon radiated in the Monte Carlo is generated with the exact first order matrix element. The scale of α_s for the LLA option is roughly the transverse momentum of the gluon bremsstrahlung, which is typically of the order of a few GeV/c, and which describes the jet multiplicities equally well at lower energies [11].

For the transformation of the partons into hadrons, the string fragmentation model, in which the hadrons are formed along a string stretched between the outgoing partons, was used. Such a model introduces correlations between the outgoing partons which are experimentally testable, and which have been found to be in agreement with the data [12, 6].

In addition to both initial state and final state radiation, particles were allowed to decay as normal, and this provided an additional source of final state photons, e.g. from π^0 decay. Background to final state radiation from particle decays is discussed in detail in the next section.

A total of 124424 $q\bar{q}$ Monte Carlo events and 11250 $\tau\bar{\tau}$ Monte Carlo events were generated at 91.25 GeV cm energy and passed through a detailed simulation [13] of the DELPHI detector. The Monte Carlo events then were passed through the full DELPHI reconstruction and analysis chain [14] in a manner identical to the real events. However, for the Monte Carlo events each final state photon was tagged as to whether its primordial origin was (a) initial state radiation (ISR), (b) final state radiation (FSR), (c) particle decay, mostly π^0's, in which the decaying particle was produced in the final state fragmentation process, or (d) tau decays. The Monte Carlo simulations did not include the possibility of interference effects between ISR and FSR processes.

The loss of isolated energetic photons because of scattering and pair production in the material in front of the HPC was determined by Monte Carlo calculations in which single photon events were generated, were passed through a fully simulated detector, and then were passed through the standard DELPHI analysis. A total of (86 ± 1)% of the photons so generated passed the photon selection criteria outlined above. This global efficiency is constant over the photon energy range studied, 8 GeV to 45 GeV.

5 Final state photon radiation

Table 1 shows the numbers of events surviving the various cuts described above as well as the numbers of events predicted by the Monte Carlo calculation for final state radiation and for the background processes: (i) initial state radiation, (ii) QCD background, e.g. π^0 decays, and (iii) residual τ decays. Figure 2 shows the energy distribution of such photons, along with the predictions of the Monte Carlo calculations. The samples of simulated $q\bar{q}$ and $\tau\bar{\tau}$ events were appropriately weighted according to their known branching fraction, and then the full sample of Monte Carlo events was normalized only to the total number of hadronic Z^0 events before any cuts were applied, other than the selection of hadronic events. Without the cut $p_T^\gamma > 5$ GeV/c, the simulations (see Ta-

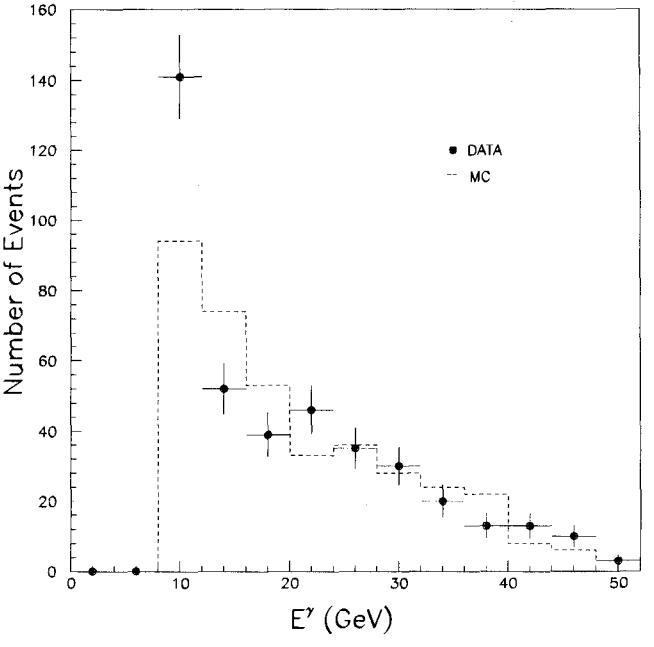

Fig. 2. Energy distribution of isolated photons in multihadronic events (points with errors) and the predictions of the Monte Carlo simulation of FSR and the background processes ISR, QCD and τ decays (dashed line)

[1] Version JETSET 7.2

Table 1. Observed isolated energetic photon events and expected contributions to the sample. The symbols Q and N refer to isolation angles of the shower with charged and neutral particles, respectively. See Sect. 3. The numbers in parentheses include the cut on transverse momentum with respect to the thrust axis

Selection	DATA observed	MC total	MC FSR	MC ISR + QCD + τ
Hadronic Z's	105876	105876 normalization		
$E_\gamma > 8$ GeV $45° < \vartheta_\gamma < 135°$ $\vartheta_\gamma < 88°$ or $> 92°$	22801	24409	317	24092
$p_T^\gamma > 5$ GeV/c	(1417)	(1408)	(176)	(1232)
ϕ fiducial cuts	22350 (1386)	23979 (1378)	313 (175)	23666 (1203)
Iso. $Q(>0.5\text{ GeV}) > 20°$	660 (313)	564 (272)	168 (147)	396 (125)
Iso. $N(>2\text{ GeV}) > 20°$	401 (262)	379 (230)	166 (146)	213 (84)

ble 1, column 5) predict 213 background events due to initial state radiation, residual τ decays, and QCD background, almost all of which is from isolated π^0 decays. This number is significantly smaller than the 401 observed photon candidates (see Table 1, column 2), and leaves 188 events due to additional sources. Photon emission from final state quarks (see Table 1, column 4) can approximately account for this difference, since the simulation of final state radiation, described in the previous section, predicts a contribution of 166 additional photons within the requisite cuts. The discrepancy is 22 events or 5%.

The QCD background from hadronic decays can be reduced further by also imposing the p_T cut described above. In this case, the observed signal is 262 events and the calculated background is 84 events, which result in 178 FSR events. The Monte Carlo simulation predicts 146 events, so the discrepancy is 32 events or 12%.

These discrepancies are not statistically significant. Nevertheless, in order to check if the residual discrepancy may be due to an inadequate description of gluon bremsstrahlung in hadronic events and to provide an estimate of the QCD background to FSR from the data themselves, the entire analysis to select isolated photons has been repeated, but it has been applied to charged particles in hadronic events. In this "charged particle analysis" electrons are removed by the isolation criteria since electrons produce electromagnetic showers in the HPC close to the charged particle track. Tau decays are largely removed by the cut $p_T > 5$ GeV/c. The simulation of tau decays indicates that only 6 τ decays survive this cut in the charged particle analysis. However, the sample of charged particles passing all the cuts does include a small component of muons which come from particle decay and not from gluon bremsstrahlung.

The p_T distribution with respect to the thrust axis of the charged particles passing all the cuts (minus the calculated contribution from tau decays) was normalized to the number of isolated photon events passing all the cuts and in the region $p_T < 5$ GeV/c, i.e. the region dominated by background (see Fig. 1), also with the calculated tau contribution removed. This normalisation is necessary because (a) a significant fraction of the charged particles are not pions, and therefore 1/2 the charged particle distribution is a poor estimate of the π^0 distribution, and (b) the probability of a charged pion passing the cuts is significantly greater than the probability of a π^0 passing the cuts because the π^0 decays into two photons, and thus its energy is shared between two particles. Often the two photons are detected in the HPC as separate electromagnetic showers, and even the more energetic photon may fail the 8 GeV energy cut. In addition, the isolation criteria may be violated.

The QCD background to final state radiation is estimated as the number of "isolated charged particle" events, appropriately normalized and with $p_T > 5$ GeV/c. This is 90 events, which when added to the expected background of 6 events from tau decays yields a total background estimate of 96 events. This number is to be compared with the background of 84 events predicted by the Monte Carlo calculations. Since the charged pions come only from quark and gluon fragmentation, the discrepancy must be in the Monte Carlo description of the fragmentation process. Because of the large systematic errors in the charged particle analysis, the calculation of the cross section for final state radiation (see next section) used the Monte Carlo calculation to estimate the background to final state radiation. The small discrepancy in the isolated photon analysis is not evidence for an anomalous production of photons, but the number of FSR events predicted by the Monte Carlo calculations is systematically below the observations. This effect has been observed in previous experiments [15], and is the subject of some theoretical study [16].

The excess of data above Monte Carlo at the low end of the photon energy spectrum (see Fig. 2), is not especially associated with data taken at a center-of-mass energy slightly above that of the Z^0 peak, and thus it probably is not due to initial state radiation. In addition, this excess remains when only data taken at a center-of-mass energy at the top of the Z^0 peak are considered, and therefore it may not be attributed to interference effects between ISR and FSR which have been neglected in the Monte Carlo calculations.

The effect of varying the isolation angle cuts on the data and Monte Carlo was studied, and agreement is

maintained with more severe isolation angle cuts. For example, the ratio data/Monte Carlo of 401/379 at 20° isolation angle cut becomes 230/221 at 30° and 190/180 at 40°. Isolation angles less than 20° result in contamination from events in which the photon is not clearly separated from a hadronic jet.

The kinematical distributions of the isolated energetic photons and the number of events observed are consistent with the hypothesis of final state radiation from the primary quarks in Z^0 decays [1]. For the selection criteria applied, the Monte Carlo studies predict that less than 0.1 photon events originate from radiation by secondary quarks.

6 Cross sections for final state radiation

In order to obtain the true number of events with final state radiation, the number of events with isolated energetic photons after all cuts (262) was corrected for the following effects:

- The remaining background from initial state radiation, QCD processes, e.g. neutral pions, and τ's, was obtained from the Monte Carlo calculation described in the previous section. This leaves after subtraction 178 ± 16 events, where the quoted error is statistical only.
- The loss of final state radiation events due to pair production and scattering in the material before the HPC. From a study of the Monte Carlo events this loss was found to be $(14 \pm 1)\%$.
- The loss of final state radiation events due to the isolation criteria (cuts d and e) after applying the p_T cut. This loss was determined by study of the Monte Carlo events to be $(16.6 \pm 3.0)\%$ of the events.
- The loss of final state radiative events due to the geometrical acceptance cuts (cuts b and f). This induces a loss of 16.7% of the events.

Additional contributions to the systematic error include the finite resolution of the measured quantities, e.g. E_γ, in the vicinity of the cuts (6%), the uncertainty in the background subtraction from fluctuations in the Monte Carlo calculations (9.5%), and a theoretical uncertainty in the number of isolated photons produced in the hadronization process (5%, see [2]).

The resulting number of corrected events is $298 \pm 27 \pm 38$. The first error is statistical and the second error systematic. This number represents the corrected number of final state radiation events with a photon energy >8 GeV, polar angle between 45° and 135° and a transverse momentum of the photon relative to the event thrust axis $p_T > 5$ GeV/c.

The cross section was computed by normalizing to the measured hadronic cross section on the Z^0 peak as reported by the DELPHI collaboration [9]. This leads to a cross section of $86.1 \pm 7.8 \pm 11.0$ pb for final state radiation in the kinematic region specified by the above cuts.

The differential cross sections as functions of the photon energy, E_γ, and transverse momentum relative to the thrust axis, p_T, are shown in Fig. 3. The background

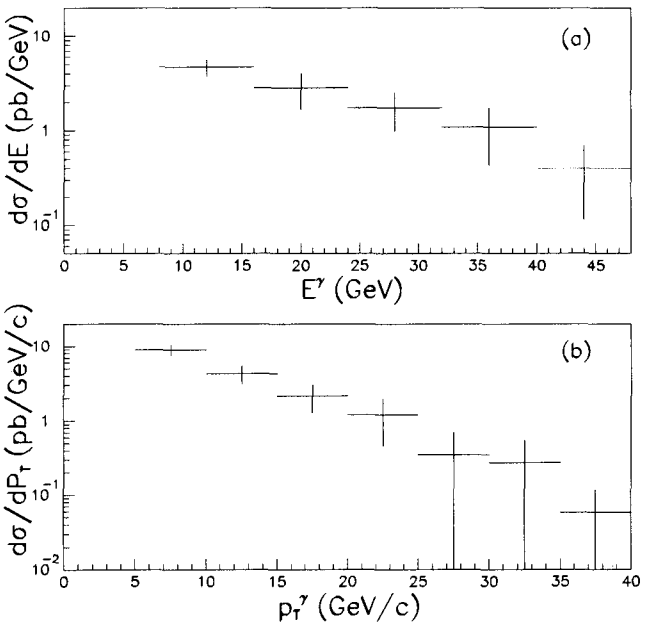

Fig. 3a, b. Differential cross section for final state radiation as a function of **a** E^γ and **b** p_T^γ relative to the thrust axis

predicted by the Monte Carlo calculation was subtracted bin by bin and the efficiency for the isolation cut was computed as a function of energy and p_T.

These measurements augment earlier results from e^+e^- experiments at LEP [15] and at center of mass energies near 30 GeV [17].

7 Quark couplings to the Z^0 boson

If all energetic isolated photons remaining after the cuts and after the background subtractions are attributed to final state radiation of primary quarks, the electroweak couplings of charge 1/3 and 2/3 quarks can be determined from the comparison of their production rate with the measured hadronic width of the Z^0 [9]. Following the notation of reference [2], the weak couplings for final state fermions f are written as

$$c_f = v_f^2 + a_f^2 \tag{1}$$

in the standard model notation the vector and axial couplings v and a are

$$v_f = 2I_{3,f} - 4Q_f \sin^2\theta_W \quad \text{and} \quad a_f = 2I_{3,f} \tag{2}$$

where I_3, Q and θ_W are the third component of the weak isospin, the charge of the quark and the weak mixing angle, respectively.

Assuming that only five quark flavours contribute, the hadronic decay width of the Z^0 is in first order QCD

$$\Gamma_{\text{had}} = N_c \frac{G_\mu M_Z^3}{24\pi\sqrt{2}} \cdot \left(1 + \frac{\alpha_s}{\pi}\right) \cdot (3c_{1/3} + 2c_{2/3}) \tag{3}$$

where N_c is the number of colors, G_μ is the muon decay constant, M_Z is the mass of the Z^0, and α_s is the strong coupling constant. The constants $c_{1/3}$ and $c_{2/3}$ are the couplings to charge 1/3 and charge 2/3 quarks respectively. The latest parameter values from the DELPHI experiment [9], $M_Z = 91.177 \pm 0.022$ GeV/c^2, $\Gamma_{had} = 1.726 \pm 0.019$ GeV, and $\alpha_s = 0.110 \pm 0.006$ an appropriate average of the results in [18] lead to

$$S_{q\bar{q}} = (3\,c_{1/3} + 2\,c_{2/3})_{had} = 6.70 \pm 0.06 \quad (4)$$

where the error is dominated by the contribution from the hadronic width.

The decay width into the final state radiative events is proportional to a different combination of the coupling constants $c_{1/3}$ and $c_{2/3}$. As the photons couple to the square of the electric charge of the quarks, the yield of radiative events remaining inside the cuts is proportional to $(3\,c_{1/3} + 8\,c_{2/3})$. Since the same cuts are applied to the real data and to the Monte Carlo, this proportionality holds for both samples and therefore

$$\frac{(3\,c_{1/3} + 8\,c_{2/3})_{exp}}{(N_{\gamma q\bar{q}})_{exp}} = \frac{(3\,c_{1/3} + 8\,c_{2/3})_{MC}}{(N_{\gamma q\bar{q}})_{MC}}. \quad (5)$$

The indices 'exp' and 'MC' refer to the experimental values and those resulting from the simulation, respectively. $(N_{\gamma q\bar{q}})_{exp}$ is the uncorrected number of events in the data after all cuts have been applied, and after the predicted number of background events (ISR + QCD + τ) have been subtracted. $(N_{\gamma q\bar{q}})_{MC}$ is the number of FSR events predicted by the Monte Carlo, normalized to the same total number of hadronic events as the data and submitted to the same cuts. This analysis includes the assumption that the relative production rate and the selection efficiencies are the same for all charge 1/3 quarks and are the same for all charge 2/3 quarks. Higher order QCD corrections are approximated by the parton shower algorithm implemented in the Monte Carlo. The result for the final state radiation is

$$S_{\gamma q\bar{q}} = (3\,c_{1/3} + 8\,c_{2/3})_{exp} = 16.6 \pm 1.5 \pm 2.1. \quad (6)$$

The first error is statistical and the second error refers to the systematic effects discussed in the previous section.

The constraints induced by the two relations (4) and (6) are displayed as two bands in Fig. 4. The crossing of the two bands determines the values of the couplings $c_{1/3}$ and $c_{2/3}$. This yields

$$c_{1/3} = v_{1/3}^2 + a_{1/3}^2 = 1.13 \pm 0.29$$

and

$$c_{2/3} = v_{2/3}^2 + a_{2/3}^2 = 1.65 \pm 0.43$$

with a correlation coefficient of -0.99. This result is consistent with the standard model prediction of $c_{1/3} = 1.48$ and $c_{2/3} = 1.15$ for $\sin^2\theta_W = 0.229$.

8 New processes producing isolated energetic photons

Since no evidence is observed of a significant excess of isolated photons in the data over that expected from standard model processes, including initial and final state radiation, limits may be placed on the existence of new phenomena. Possible new processes considered in this analysis are (a) the decay of the Z^0 into a Higgs boson

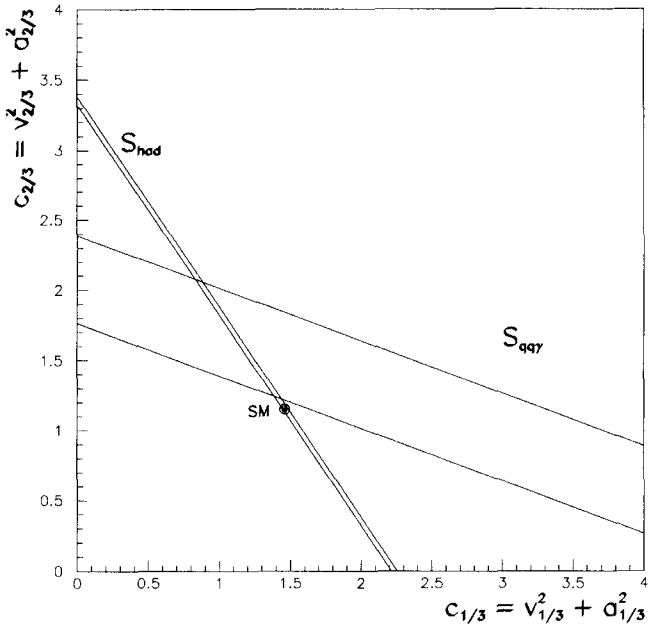

Fig. 4. Correlation of the couplings for charge 1/3 and charge 2/3 quarks. Also shown is the expectation from the standard model (black point)

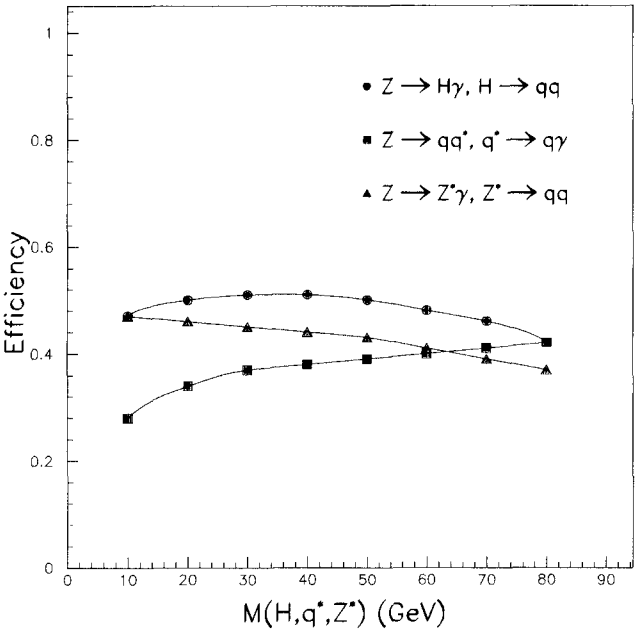

Fig. 5. Overall efficiency as functions of intermediate particle mass for ● $\sigma(e^+e^- \to Z^0 \to H + \gamma)$. BR($H \to$ hadrons), ■ $\sigma(e^+e^- \to Z^0 \to q^* +$ hadrons). BR($q^* \to \gamma +$ hadrons), and ▲ $\sigma(e^+e^- \to Z^0 \to \gamma + Z^*)$. BR($Z^* \to$ hadrons)

and a photon, (b) an excited quark, q^*, which decays into a normal quark q and a photon, and (c) the decay of the Z^0 boson into a photon and normal hadronic matter. This last case is possible only if the Z^0 were a composite particle. In that case the coupling $ZZ^*\gamma$ would be allowed.

In each of these three cases the final state consists of an isolated photon and the fragmentation products of the quark and antiquark. Total efficiencies for these three processes were calculated by Monte Carlo methods, and are shown in Fig. 5 as functions of the hypothetical intermediate particle mass, i.e. Higgs, q^*, and Z^*. For cases (a) and (b) a production angular distribution of $1+\cos^2\vartheta$, where ϑ is the polar angle with respect to the beam axis of the Higgs [19] or the q^*, was assumed. Case (c) is discussed below.

The calculations include all effects due to geometric acceptances, fiducial cuts, isolation criteria, and additional losses of photons due to the presence of material in front of the HPC. For these analyses, the cut shown in Table 1, i.e. $p_T^\gamma > 5$ GeV/c, is not applied as such a cut would seriously reduce the expected signals. Thus, the observed number of events for this analysis is 401.

The process $Z^0 \to \text{Higgs} + \gamma$ is forbidden to occur through a $ZH\gamma$ coupling in the standard model. However, the occurrence of fermion and W boson loops can provide an effective coupling for the process $Z^0 \to \text{Higgs} + \gamma$. This process has been studied in detail for $m_t = 60$ GeV and $m_t = 200$ GeV [3]. Calculation of the width is dominated by contributions from the W boson loops.

In order to improve the resolution the constraints of conservation of energy and momentum have been imposed on the data. This is done by rescaling the final state photon and quark momenta. The procedure is as follows: (1) The Lund jet-finding algorithm is invoked, insisting on precisely two hadronic jets for all the final state particles except the isolated photon, in order to estimate approximately the final state quark and antiquark momenta. In general, the 3-momenta of the photon and the two quarks do not sum to zero because of measurement errors and missing particles from the quark fragmentation process, e.g. neutrinos, K^0's, neutrons, and other particles which escape detection. Monte Carlo calculations indicate that neutrinos and lost hadrons account for most of the discrepancy in e.g. coplanarity. (2) Conservation of 3-momentum is imposed by fixing the photon momentum and moving the two jet momenta only. (3) All three momenta are rescaled to the known center of mass energy, neglecting the quark rest masses. The distribution in the ratio of scaled to raw photon energies is a gaussian with a sigma of 0.3%, but which also has a small tail which extends up to 4.0%. This method has been shown to reproduce Monte Carlo simulations more accurately than simple rescaling because it does not attribute too much of the hadronic losses to the relatively well-measured photon. The mass distributions described below use the rescaled variables, but differences with the raw distributions are slight. In particular, the $q\bar{q}$ mass distribution is essentially unaffected by the rescaling.

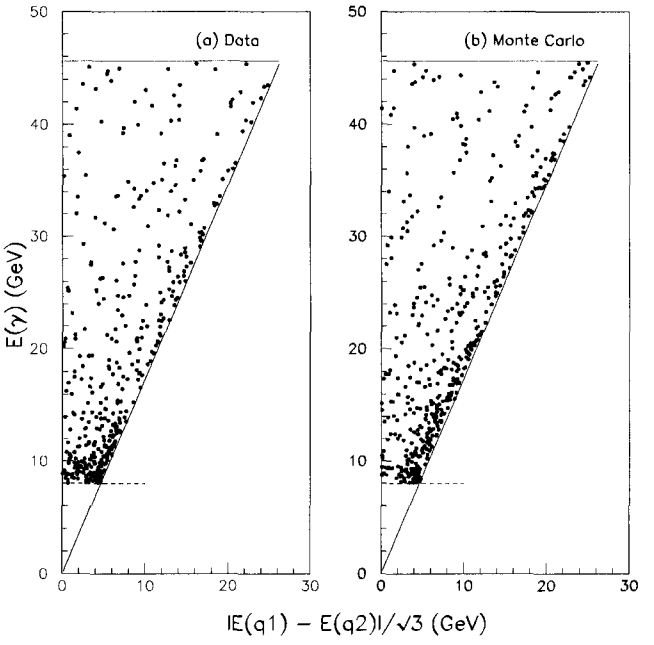

Fig. 6a, b. Dalitz plots: E_γ vs. $|E_{q1}-E_{q2}|/\sqrt{3}$ for **a** data and **b** Monte Carlo simulation. The dotted line indicates the cut $E_\gamma > 8$ GeV

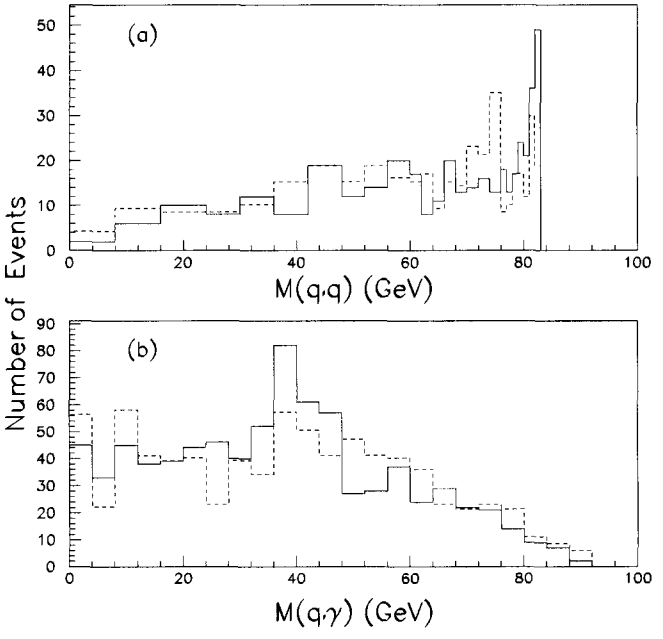

Fig. 7a, b. Distributions in invariant mass **a** $M(q, \bar{q})$, and **b** $M(q, \gamma)$ (two combinations per event). The dashed lines indicate the predictions of the Monte Carlo simulation

In Fig. 6 the Dalitz plots, E_γ vs. $|E_{q1}-E_{q2}|/\sqrt{3}$, for (a) data and (b) Monte Carlo simulation is shown. The Monte Carlo events shown in Fig. 6b have not been normalized to the data, and thus appear with enhanced 'statistics'. In Fig. 7a the measured distribution in $q\bar{q}$ invariant mass, i.e. in the missing mass recoiling against the measured photon, is shown. In Fig. 7b the measured $q\gamma$ invariant mass distribution (two combinations per

event) is shown. From the Dalitz plot it is clear that apparent structures in the mass distributions are seen to be kinematical reflections of the cut $E_\gamma > 8$ GeV and of the distribution of data which is dominantly at the low end of the photon energy spectrum.

The resolution in the $q\bar{q}$ invariant mass is determined directly from the resolution on the measured photon energy, and it varies from less than 1 GeV at 80 GeV mass to 8 GeV at 35 GeV mass. The variable bin width in Fig. 7a reflects this resolution.

The resolution in the $q\gamma$ invariant mass was determined by Monte Carlo methods. The $q\gamma$ invariant mass, as calculated from the final (detector modified) variables, was compared with the $q\gamma$ invariant mass as calculated from the generated variables. In each case the full analysis described above, including momentum rescaling, was reproduced. The resolution is better than 4 GeV, essentially independent of $q\gamma$ mass, over the full kinematic range.

Since no excess of energetic isolated photons is observed beyond that expected from initial and final state radiation plus QCD background, an upper limit may be determined of the product of the cross section for the reaction $\sigma(e^+e^- \to Z^0 \to \text{Higgs} + \gamma)$ times the branching fraction BR(Higgs $\to q\bar{q}$). The limit at the 95% confidence level is shown in Fig. 8 as a function of the Higgs mass. This limit is more than an order of magnitude above the prediction of the standard model with a single Higgs doublet.

An excited quark q^* could be produced at LEP with relatively large mass, e.g. with $M_{q^*} < M_Z - M_{\bar{q}}$ in the reaction $Z^0 \to q^*\bar{q}$. An upper limit at the 95% confidence level of the product of the cross section for the reaction $\sigma(e^+e^- \to Z^0 \to \bar{q}q^*)$ times the branching fraction BR($q^* \to q\gamma$) may thus be determined, and this limit is also shown in Fig. 8. This result significantly extends the previous limits [15, 20].

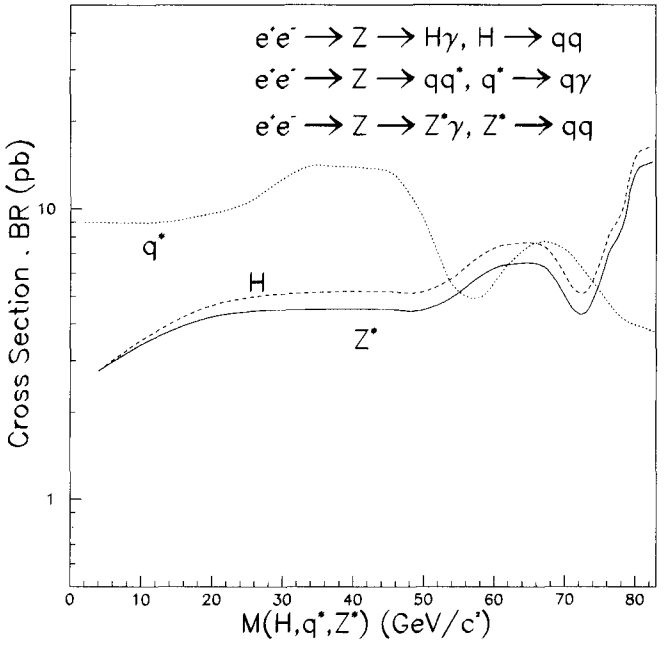

Fig. 8. Figure 8: Cross section times branching ratio upper limits at the 95% confidence level for $\sigma(e^+e^- \to Z^0 \to H + \gamma) \times \text{BR}(H \to \text{hadrons})$, $\sigma(e^+e^- \to Z^0 \to q^* + \text{hadrons}) \times \text{BR}(q^* \to \gamma + \text{hadrons})$, and $\sigma(e^+e^- \to Z^0 \to \gamma + Z^*) \times \text{BR}(Z^* \to \text{hadrons})$

If the Z^0 were a composite particle, made up of charged constituents, it could decay directly into a photon plus hadrons. Possibilities include (a) anomalous three- and four-boson couplings [21], which would produce a broad spectrum of photon energies, (b) Z^0 decay into a photon and an off-mass-shell Z, here called Z^*, which would also produce a broad spectrum of photon energies, and (c) Z^0 decay into a photon and a scalar partner S, which could produce a nearly monochromatic photon signal, provided the width of the S is not too large.

The kinematic configurations of the decay are in each case model dependent. For case (b), an isotropic decay of the Z^0 into a photon and a vector boson (here called Z^*) was assumed. The angular distribution $1 + \cos^2 \vartheta^*$ was assumed for the Z^* decay into $q\bar{q}$, where ϑ^* is the Gottfried-Jackson angle of the Z^* decay into $q\bar{q}$, i.e. the angle of the q momentum in the $q\bar{q}$ rest frame with respect to the $q\bar{q}$ momentum in the Z^0 rest frame.

The overall efficiency for such events, as determined in the Monte Carlo simulation, and as a function of Z^* mass, was shown in Fig. 5. In Fig. 7a the invariant mass distribution of the missing mass against the photon, i.e. the $q\bar{q}$ mass, was shown, and was consistent with conventional processes. The upper limit at the 95% confidence level of such an anomalous process may thus be determined. The result, as a function of Z^* mass, is also shown in Fig. 8.

The absence of any narrow structures in the $q\bar{q}$ invariant mass distribution effectively argues against case (c), i.e. the decay of the Z^0 into a photon and a narrow scalar, S. Case (a) has limits very close to those of case (b) as the two cases may differ only in a small change in the angular distribution.

9 Conclusions

The measured production cross section, energy and transverse momentum spectra of isolated photons with $E_\gamma > 8$ GeV are compatible with the hypothesis of final state radiation from primary quarks plus background processes predicted by the standard model (ISR + QCD + τ decays). This measurement, when combined with measurement of the hadronic width of the Z^0, determines the quark couplings to the Z^0. Specifically, the couplings of up-type and down-type quarks are determined to be:

$$v_{1/3}^2 + a_{1/3}^2 = 1.13 \pm 0.29 \quad \text{and} \quad v_{2/3}^2 + a_{2/3}^2 = 1.65 \pm 0.43.$$

There is no evidence for anomalous production of photons. This leads to the measurement of the differential cross section for final state radiation (see Fig. 3), and to the determination of upper limits at the 95% confidence level on the production cross section times branching fraction for three processes: (a) $\sigma(e^+e^- \to Z^0 \to H + \gamma)$.

BR($H \to$ hadrons), (b) $\sigma(e^+ e^- \to Z^0 \to q^* +$ hadrons). BR($q^* \to \gamma + q$), and (c) $\sigma(e^+ e^- \to Z^0 \to \gamma + Z^*)$. BR($Z^* \to$ hadrons), as shown in Fig. 8.

Acknowledgments. We are greatly indebted to our technical collaborators and to the funding agencies for their support in building and operating the DELPHI detector, and to the members of the CERN-SL Division for the superb performance of the LEP collider.

References

1. T.F. Walsch, P. Zerwas: Phys. Lett. 44B (1973) 195; S.J. Brodsky, C.E. Carlson, R. Suaya: Phys. Rev. D14 (1976) 2264; K. Koller, T.F. Walsh, P. Zerwas: Z. Phys. C – Particles and Fields 2 (1979) 197; E. Laermann, T.F. Walsh, I. Schmitt, P.M. Zerwas: Nucl. Phys. B207 (1982) 205
2. P. Mättig, W. Zeuner: Z. Phys. C – Particles and Fields 52 (1991) 31
3. R.N. Cahn, M.S. Chanowitz, N. Fleishon: Phys. Lett. 82B (1979) 113; L. Bergström, G. Hulth: Nucl. Phys. B259 (1985) 137; A. Barroso, J. Pulido, J.C. Romão: Nucl. Phys. B267 (1986) 509; P.J. Franzini et al., in: Proceedings of the Workshop on Z Physics at LEP I, ed. G. Altarelli, R. Kleiss, C. Verzegnassi, p. 59 CERN 89-08 (1989) Vol. 2
4. F. Boudjema, F.M. Renard, in: Proceedings of the Workshop on Z Physics at LEP I, ed. G. Altarelli, R. Kleiss, C. Verzegnassi, CERN 89-08 (1989)
5. DELPHI Coll., P. Aarnio et al.: Nucl. Instrum. Methods A303 (1991) 233
6. DELPHI Coll., P. Aarnio et al.: Phys. Lett. 240B (1990) 271
7. H.G. Fischer: Nucl. Instrum. Methods A265 (1988) 218; F.L. Navarria et al.: Nucl. Instrum. Methods A257 (1987) 499; A. Cattai et al.: Nucl. Instrum. Methods A235 (1985) 310; E.I. Rosenberg: The DELPHI high density projection chamber, Proceedings of the gas sampling calorimetry workshop II, Fermilab, Batavia, Il. (1985) 450; H.G. Fischer, O. Ullaland: IEEE Trans. Nucl. Sci. NS-27 (1980) 38
8. H.B. Crawley et al.: IEEE Trans. Nucl. Sci. NS-35 (1988) 295; H.B. Crawley et al.: IEEE Trans. Nucl. Sci. NS-34 (1987) 261
9. DELPHI Coll., P. Aarnio et al.: Phys. Lett. 231B (1989) 539; DELPHI Coll., P. Abreu et al.: Phys. Lett. 241B (1990) 435; DELPHI Coll., P. Abreu et al.: CERN-PPE/90-119, Submitted to XV International Conference on High Energy Physics, Singapore, August 1990; DELPHI Coll., P. Abreu et al.: Nucl. Phys. B 367 (1991) 551
10. T. Sjöstrand: Comput. Phys. Commun. 27 (1982) 243; T. Sjöstrand: Comput. Phys. Commun. 28 (1983) 229; T. Sjöstrand: Comput. Phys. Commun. 39 (1986) 347; T. Sjöstrand, M. Bengtsson: Comput. Phys. Commun. 43 (1987) 367; JETSET version 7.2
11. S. Bethke: Z. Phys. C – Particles and Fields 43 (1989) 331; N. Magnussen, PhD thesis, Univ. of Wuppertal, 1988, DESY F22-89-01; AMY Coll., I.H. Park et al.: Phys. Rev. Lett. 62 (1989) 1713; MARK-II Coll., S. Bethke et al.: Z. Phys. C – Particles and Fields 43 (1989) 325; OPAL Coll., M.Z. Akrawy et al.: Phys. Lett. 235B (1990) 389; TASSO Coll., W. Braunschweig et al.: Phys. Lett. 214B (1988) 286
12. Z. Kunszt, P. Nason, in: Proceedings of the Workshop on Z physics at LEP I, ed. G. Altarelli, R. Kleiss, C. Verzegnassi, p. 373 CERN 89-08 (1989) Vol. I
13. DELPHI Simulation program: DELSIM User Manual, DELPHI 87-96 PROG-99, Geneva, 1989; DELSIM Reference Manual, DELPHI 87-98 PROG-100, Geneva, 1989
14. DELPHI Reconstruction program: DELANA User Guide, DELPHI 87-44 PROG-137, Geneva, 1989
15. OPAL Coll., M.Z. Akrawy et al.: Phys. Lett. 246B (1990) 285; OPAL Coll., G. Alexander et al.: Phys. Lett. 264B (1991) 219; ALEPH Coll., D. Decamp et al.: Phys. Lett. 264B (1991) 476; L3 Coll., B. Adeva et al.: Phys. Lett. 262B (1991) 155
16. G. Kramer, B. Lampe: QCD corrections to final state photon bremsstrahlung in $e^+ e^-$ annihilation, DESY 91-078, 1991
17. MAC Coll., E. Fernandez et al.: Phys. Rev. Lett. 54 (1985) 95; JADE Coll., W. Bartel et al.: Z. Phys. C – Particles and Fields 28 (1985) 343; TASSO Coll., W. Braunschweig et al.: Z. Phys. C – Particles and Fields 41 (1988) 385; JADE Coll., D.D. Pitzl et al.: Z. Phys. C – Particles and Fields 46 (1990) 1
18. DELPHI Coll., P. Abreu et al.: Phys. Lett. 247B (1990) 167; DELPHI Coll., P. Abreu et al.: Phys. Lett. 252B (1990) 149
19. G. Ridolfi, private communication
20. CELLO Coll., H.J. Behrend et al.: Phys. Lett. 181B (1986) 178
21. F.M. Renard: Phys. Lett. 116B (1982) 269; F.M. Renard: Phys. Lett. 132B (1983) 449; F.M. Renard: Nucl. Phys. B196 (1982) 93; G. Gounaris et al.: Phys. Lett. 137B (1984) 261; V. Barger et al.: Phys. Rev. D30 (1984) 1513 (Sect. D, (2.14)–(2.18)); K. Hagiwara et al.: Nucl. Phys. B282 (1987) 253 (Appendix D); and H. Czyz, K. Kolodziej, M. Zralek: Z. Phys. C – Particles and Fields 43 (1989) 97